

Optimization of metal-clad waveguides for sensitive fluorescence detection

Aldo Minardo¹, Romeo Bernini², Flavio Mottola¹ and Luigi Zeni¹

¹*Dipartimento di Ingegneria dell'Informazione – Seconda Università di Napoli
Via Roma, 29, 81031 Aversa, Italy
aldo.minardo@unina2.it, flavio.mottola@unina2.it, zeni@unina.it*

²*Istituto per il Rilevamento Elettromagnetico dell'Ambiente
Consiglio Nazionale delle Ricerche, Via Diocleziano, 328 – 80124, Naples, Italy
bernini.r@irea.cnr.it*

Abstract: Recently, metal-clad leaky waveguides (MCLW) have been proposed as highly sensitive single point sensor devices for small-volume refractive index (RI) and fluorescence detection. In this paper, we present a theoretical study of the efficiency of MCLW-based sensors on glass substrate, for fluorescence detection. It is shown that MCLWs can be designed in order to obtain an efficient coupling of fluorescence emission with their leaky modes. This leads to a higher directionality of the fluorescence emission into the glass substrate, when compared to the emission near a pure glass/water interface and surface-plasmon coupled emission (SPCE). Numerical analyses also indicate that collecting the fluorescence emission through a water-immersed microscope objective, may result in a 70-fold enhancement of the detectable signal when compared to conventional fluorescence detection carried out on a glass slide.

©2006 Optical Society of America

OCIS codes: (260.2110) Electromagnetic theory; (300.6280) Spectroscopy, fluorescence and luminescence

References and Links

1. Hirschfeld, "Total reflection fluorescence," *Can. Spectroscopy* **10**, 128 (1965).
2. T. Ruckstuhl, M. Rankl, and S. Seeger, "Highly sensitive biosensing using a supercritical angle fluorescence (SAF) instrument," *Biosens. Bioelectron.* **18**, 1193-1199 (2003).
3. G. Stengel, W. Knoll, "Surface plasmon field-enhanced fluorescence spectroscopy," *Nucleic Acids, Res.* **33**, e69 (2005).
4. J. R. Lakowicz, "Radiative decay engineering 3. Surface plasmon-coupled directional emission," *Anal. Biochem.* **324**, 170-182 (2004).
5. I. Gryczynski, J. Malicka, Z. Gryczynski, and J. R. Lakowicz, "Radiative decay engineering 4. Experimental studies of surface plasmon-coupled directional emission," *Anal. Biochem.* **324**, 170-182 (2004).
6. W. Weber and C. Eagen, "Energy transfer from an excited dye molecule to the surface plasmons of an adjacent metal," *Opt. Lett.* **4**, 236- (1979),
<http://www.opticsexpress.org/abstract.cfm?URI=OPEX-4-8-236>.
7. C. D. Geddes, I. Gryczynski, Z. Gryczynski, "Directional surface plasmon coupled emission," *J. Fluoresc.* **14**, 119-123 (2004).
8. F. D. Stefani, K. Vasilev, N. Bocchio, N. Stoyanova, M. Kreiter, "Surface-plasmon-mediated single-molecule fluorescence through a thin metallic film," *Phys. Rev. Lett.* **94**, 023005 (2005).
9. J. Enderlein and T. Ruckstuhl, "The efficiency of surface-plasmon coupled emission for sensitive fluorescence detection," *Opt. Express* **13**, 8855-8865 (2005),
<http://www.opticsexpress.org/abstract.cfm?URI=OPEX-13-22-8855>.
10. E. Matveeva, J. Mailcka, I. Gryczynski, J. R. Lakowicz, "Multi-wavelength immunoassays using surface plasmon-coupled emission," *Biophys. Biochem. Res. Comm.* **313**, 721-726 (2004).
11. J. Enderlein, "Single-molecule fluorescence near a metal layer," *Chem. Physics* **247**, 1-9 (1999).
12. M. Zourob, S. Mohr, B. J. Treves Brown, P. R. Fielden, M. McDonnell, N. J. Goddard, "The development of a metal clad leaky waveguide sensor for the detection of particles," *Sens. and Act. B* **90**, 296-307 (2003).
13. M. Zourob, N. J. Goddard, "Metal clad leaky waveguides for chemical and biosensing applications," *Biosensors and Bioelectronics* **20**, 1718-1727 (2005).

14. M. Zourob, S. Mohr, P. R. Fielden N. J. Goddard, "Small-volume refractive index and fluorescence sensor for micro total analytical system (μ -TAS) applications," *Sens. and Act. B* **94**, 304-312 (2003).
15. J. Enderlein, "Fluorescence detection of single molecules near a solution/glass interface—an electrodynamic analysis," *Chem. Phys. Lett.* **308**, 263-266 (1999).
16. J. Enderlein, "Theoretical study of detection of a dipole emitter through an objective with high numerical aperture," *Opt. Lett.* **25**, 634-636 (2000), <http://www.opticsexpress.org/abstract.cfm?URI=OPEX-25-9-634>.
17. R. R. Chance, A. Prock, R. Silbey, "Molecular fluorescence and energy transfer near interfaces," *Adv. Chem. Phys.* **37**, 1-65 (1978).
18. J. Enderlein, "A theoretical investigation of single-molecule fluorescence detection on thin metallic layers," *Biophysical Journal* **78**, 2151-2158 (2000).
19. M. Born, E. Wolf, *Principles of optics, Electromagnetic Theory of Propagation, Interference and Diffraction of Light*, 7th (Cambridge University Press, 1999), p. 65.
20. N. J. Harrick, *Internal Reflection Spectroscopy*, (Interscience New York, 1967).
21. N. Skivesen, R. Horvath, and H. C. Pedersen, "Optimization of metal-clad waveguide sensors," *Sens. and Act. B* **106**, 668-676 (2005).
22. H. Choumane, N. Ha, C. Nelep, A. Chardon, G. O. Reymond, C. Goutel, G. Cerovic, F. Vallet, and C. Weisbuch, "Double interference fluorescence enhancement from reflective slides: Application to bicolor microarrays," *App. Phys. Lett.* **87**, 031102 (2005).
23. W. Lukosz, "Light-emission by magnetic and electric dipoles close to a plane dielectric interface. 3. radiation-patterns of dipoles with arbitrary orientation," *J. Opt. Soc. Am.* **69**, 1495-1503 (1979).

1. Introduction

Fluorescence detection is now a dominant method for high-sensitivity detection in a wide range of biotechnology applications, including gene expression, polymerase chain reaction, medical diagnostics, forensics, and increasingly for biohazard detection. In all these applications there is a need for increased sensitivity to allow detection of a small number of target molecules. An additional requirement in these assays is the surface selectivity of the detection technique, i.e. the possibility that background fluorescence from the bulk solution is efficiently suppressed in comparison with fluorescence generated by surface-captured molecules. A widely employed technique for achieving such surface-selectivity is total internal-reflection fluorescence (TIRF) excitation [1]. In TIRF, fluorescence is excited by using the evanescent wave formed upon total internal reflection of light at the interface separating two media of different refractive indexes. As evanescent field typically extends in the aqueous medium for a fraction of the excitation wavelength, only surface-bound fluorophores will be excited and contribute to the detected fluorescence.

Recently, several alternative approaches have been proposed with the goal of achieving effective surface-restricted fluorescence detection without compromising the signal-to-background ratio, namely supercritical angle fluorescence (SAF) [2], surface plasmon field-enhanced fluorescence (SPFS) [3] and surface plasmon-coupled emission (SPCE) [4-5]. In these techniques, surface selectivity is achieved by exploiting the different emission characteristics of fluorescence light emitted near a surface, with respect to bulk fluorescence. Among these techniques, SPCE has attracted a particular interest, as it was introduced as an extremely powerful and straightforward new method for sensitive detection in analytical chemistry. The core idea of SPCE is the use of a semi-transparent metal film that is deposited on a glass surface to enhance fluorescence excitation and to improve fluorescence collection for molecules close to the surface. It is well-known that for plane wave illumination from the glass side at an incident angle close to the angle of surface-plasmon resonance (SPR), the local electric field intensity near the surface can be significantly enhanced compared to a similar configuration without metal. It was also shown that fluorescence emission can couple into the surface plasmon (SP) mode of the metal film and subsequently be re-radiated into the glass around angles near the SPR angle [6-7]. Even single molecule detection has been reported using SPCE [8]. Although SPCE has raised expectations of improved fluorescence excitation and detection, recent theoretical studies have shown that the presence of the metal film does not enhance the detectable fluorescence signal indeed, when compared with conventional fluorescence detection on pure glass [9]. Actually, SPCE is accompanied by a high degree of energy dissipation in the metal film, so that significantly less energy is coupled

through a metal film into the glass than in the case where no metal film is present. On the other hand, SPCE offers some benefits with respect to conventional fluorescence detection. First, the fluorescent signal is highly directional into the glass, i.e. the emission is confined around a well defined angle [7]. This may help to better discriminate between fluorescence and any other background which does not show a similar directionality in emission (potentially Rayleigh and Raman scattering). Second, the angular position of the SPCE emission peak is strongly wavelength dependent (due to the strong dispersion of metals), which makes it possible to use SPCE as a spectrally resolving technique [10]. This makes parallel detection of spectrally different fluorophores possible without the use of additional dispersive elements. Third, SPCE emission is highly polarized, in contrast to emission generated at a glass/water interface [5]. These polarization properties of SPCE emission may be useful under special circumstances. Fourth, the metal film enhances the de-excitation rate of the fluorophores, thus leading to an increased photostability of the fluorophores themselves [11]. This is particularly important in experiments where a single or a few molecules are to be detected, the most relevant quantity being in this case the total number of photons which is emitted by each molecule until photobleaching occurs.

The above considerations suggest that an opportune geometry for fluorescence detection would be desirable, where the beneficial SPCE properties are kept, while increasing the detectable fluorescent signal. In this paper, we study the fluorescence emission of fluorophores emitting close to a multilayer structure, which consists of a glass substrate coated with a thin semi-transparent metal film, followed by a thin dielectric film. The latter is supposed to have a refractive index lower than the index of the glass substrate, but higher than the external aqueous medium. Hence, light can be partially confined inside of it, because total internal reflection can occur only at the film/water interface. At the lower interface, light is partially reflected by the semitransparent metal film, so that a fraction of electromagnetic energy escapes from the structure at each reflection. Due to the partial light confinement, the corresponding waveguide is said to be leaky [12], and propagation can occur only over a short distance (in the μm -range). Metal-clad leaky waveguides have recently attracted a great interest because of their enhanced sensing capabilities with respect to traditional waveguides based on high refractive index guiding films [13]. Enhanced sensitivity comes from the deeper penetration of the evanescent field inside the sensing medium, as the metal film pushes the waveguide mode further into the sensing region. Therefore, MCLWs have been proposed as efficient sensing devices for refractive index (RI) measurements, particle and fluorescence detection, in chemical and biosensing applications [12-14]. In this paper, we theoretically study the fluorescence emission of emitting dipoles placed in proximity of a metal clad waveguide. We use the term "waveguide", although we will not consider fluorescence collection through the dielectric film, as the high attenuation loss of the leaky mode would make the fluorescence signal hardly measurable. Instead, we will mainly focus on fluorescence collection through the substrate glass. We will demonstrate that the geometrical parameters of the waveguide can be chosen so as to achieve a high directionality of fluorescence emission into glass. Such emission property can be explained in terms of coupling between the emitted fluorescence and the MCLW leaky modes. When this coupling occurs, fluorescence is radiated through the glass at well-defined angles from the normal axis, each corresponding to the de-coupling angle of a mode supported by the MCLW. The thickness of the dielectric film can be chosen so that the MCLW only supports the fundamental TE mode, in that case emission into glass will occur around a single direction. Additionally, the dielectric film serves as a spacer between the fluorescing molecules and the metal surface, thereby eliminating direct quenching of molecules in close proximity to the metal. When exciting the fluorescing molecules from the glass side, we will show that strong local electric field enhancement can be achieved, eventually resulting in a 4-fold enhancement of the detectable fluorescence signal with respect to detection on a standard glass slide. It will be also shown that an even stronger enhancement can be achieved by collecting the fluorescence through a water-immersed microscope objective placed above the MCLW, although in this case the detected fluorescence radiation will not be highly directional. Even

though the possibility to employ a MCLW as an optical sensor device for fluorescence detection has been already proposed [14], to the best of our knowledge no theoretical study was previously performed studying the emission properties and detection efficiency offered by this structure.

2. Theoretical background

The theoretical treatment is based on a semi-classical approach, which considers a fluorescing molecule as an ideal dipole emitter. The optical detection properties of interest are calculated by using the emission of dipole emitters in front of a planar surface. Here, we will follow the notation of Ref. [15] for the evaluation of the emission properties of dipole emitters. The configuration under study is depicted in Fig. 1 and consists of a molecule placed in water above a glass substrate coated with a thin metal film (thickness dm) and a thin dielectric film (thickness df). The quantities of particular interest in our study are: the angular distribution of radiation (ADR) in the water half space S_w , the ADR in the glass half space S_g , and the total power S_{total} emitted by the molecule. In general, all these quantities will not only depend on the emission angles, but also on the orientation of the molecule's dipole and its distance from the dielectric film surface. Furthermore, due to the presence of the metal film, the sum of integrals of S_w and S_g over all emission angles will be smaller than S_{total} ; the difference is due to fact that part of the emitted power is absorbed and dissipated by the metal [6].

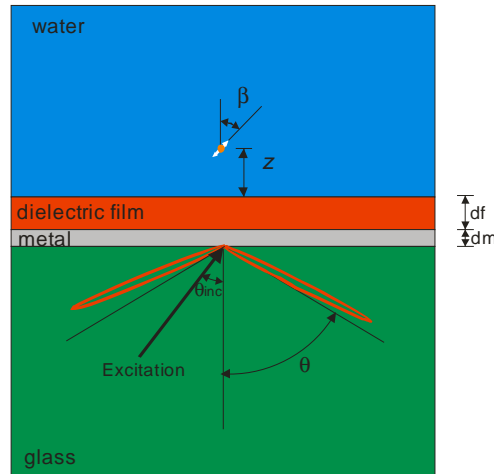


Fig. 1. Setup of MCLW-coupled emission: An aqueous solution of fluorescing molecules is placed in top of a thin dielectric film and a thin silver film deposited on glass. Fluorescence excitation is performed from the glass side by a plane wave with incident angle assuring maximum transmittivity. A single molecule is depicted as a dipole emitter with a distance z from the dielectric surface and forming an angle β with the vertical (optical) axis. The angular distribution of radiation into glass is depicted as a red curve and is a function of angle θ .

We will consider, for the sake of simplicity, a molecule with a fluorescence quantum yield (QY) equal to unity. We denote by θ the angle between the direction of emission and the vertical axis (perpendicular to the surface), and by ϕ the angle around this axis. For the planar geometry of Fig. 1, we can take for S_w and S_g the simple form used in Ref. [9]:

$$S_{w,g}(\theta, \phi, z, \beta) = S_{w,g}^{\perp}(\theta, z) \cos^2 \beta + \left[S_{w,g}^{\parallel,x}(\theta, z) \cos^2 \phi + S_{w,g}^{\parallel,y}(\theta, z) \sin^2 \phi \right] \sin^2 \beta, \quad (1)$$

where β is the angle between the dipole axis and the vertical axis, z is the dipole's distance from the dielectric film/water interface, and $S_{w,g}^\perp$ and $S_{w,g}^\parallel$ are functions of θ and z only. For $S_{total}(z, \beta)$, a similar relation holds [9]:

$$S_{total}(z, \beta) = S_{total}^\perp(z) \cos^2 \beta + S_{total}^\parallel(z) \sin^2 \beta, \quad (2)$$

The expressions of S_g , S_w , and S_{total} , for a generic dipole orientation can be derived by adopting a plane-wave integral representation of the electric field amplitude \mathbf{E}_D of the fluorescing molecule emission field, and using the appropriate multilayer Fresnel coefficients for the structure represented in Fig. 1. The ADR expressions are reported in different papers by Enderlein, Refs. [15-16], so here we do not report them for brevity. However, it is worth spending a few words about the calculation of the total emission rate S_{total} . According to the Chance, Prock, Silbey (CPS) theory [17], the total power radiated by the dipole can be determined by considering the back-reaction field \mathbf{E}_R generated by the interaction of the free field, i.e. the electric field of an emitting free dipole embedded within a homogeneous medium with refractive index n_w , with the multilayer structure formed by the glass, the metal film and the dielectric film. This back-reaction field performs work on the dipole, which may enhance or suppress the dipole emission. The total emission rate S_{total} is then the sum of the emission rate of the free dipole, $S_0 = \omega n_w k_0^3 P^2 / 3$, plus a contribution of \mathbf{E}_R on the dipole, and is given by [11]:

$$S_{total}(z) = \frac{\omega n_w k_0^3 P^2}{3} + \frac{\omega}{2} \mathbf{p} \cdot \text{Im} \mathbf{E}_R(z). \quad (3)$$

where \mathbf{p} is the dipole moment amplitude, k_0 is the vacuum wave vector amplitude of light, $k_0 = \omega/c$, ω is the oscillation frequency of the dipole, c is the vacuum speed of light, and $\mathbf{E}_R(z)$ is the back-reaction field amplitude at the dipole's position.

The probability density that a photon is emitted along the direction (θ, ϕ) is given by the ratio $S_{w,g}(\theta, \phi, z, \beta) / S_{total}(z, \beta)$, where the index, w , refers to the water half space and the index, g , to the glass half space. In what follows we will consider only the special cases of vertical ($\beta = 0$) and horizontal ($\beta = \pi/2$) dipole orientation – the general case can be easily derived using Eqs. (1-2). The efficiency of fluorescence collection through the glass can be calculated as the percentage of the total radiated energy which is emitted into glass, given by:

$$I_g^{\perp, \parallel}(z) = 2\pi \int_0^{\pi/2} d\theta \sin \theta \frac{S_g^{\perp, \parallel}(\theta, z)}{S_{total}^{\perp, \parallel}(z)}, \quad (4)$$

where $S_g^\parallel = (S_g^{\parallel, x} + S_g^{\parallel, y})/2$ and the superscript \perp refers to the vertical dipole orientation, and the superscript \parallel to the horizontal dipole orientation.

Analogously, when fluorescence is detected by a light collecting microscope objective with numerical aperture NA, immersed into water, collection efficiency can be calculated as:

$$I_w^{\perp, \parallel}(z) = 2\pi \int_0^{\theta_{\max}} d\theta \sin \theta \frac{S_w^{\perp, \parallel}(\theta, z)}{S_{total}^{\perp, \parallel}(z)}, \quad (5)$$

where θ_{\max} is the angle of the light cone seen by the objective, $\theta_{\max} = \sin(NA/n_w)$.

The energy absorbed and dissipated within the metal film can be calculated as the difference

$$I_{diss}^{\perp,\parallel}(z) = S_{total}^{\perp,\parallel}(z) - 2\pi \int_0^{\pi/2} d\theta \sin \theta \left[S_g^{\perp,\parallel}(\theta, \phi, z) + S_w^{\perp,\parallel}(\theta, \phi, z) \right] \quad (6)$$

For obtaining a final expression of the detected fluorescence emission intensity, the results for the fluorescence collection efficiency have to be combined with the efficiency with which fluorescence is excited. This needs some additional information about the molecule's dipole orientation during excitation and fluorescence emission. Here we will make the simple and experimentally most interesting assumption that the characteristic time of rotational diffusion of the molecule is much faster than the fluorescence excitation time, which means that, at the moment of fluorescence emission, any information about the initial absorption dipole orientation is lost [18]. Furthermore, in our calculations we will assume that fluorescence is excited by illuminating from the glass side, in similarity to the Kretschman configuration employed in surface plasmon resonance [5]. For a plane wave incident from the glass side under an incident angle θ_{inc} , the exciting electric field above the dielectric film surface is given by [19]:

$$T_{j0} = \frac{t_j^{gm} t_j^{mdw}}{\exp(-jk_{zm}d_m) + r_j^{gm} r_j^{mdw} \exp(jk_{zm}d_m)} \quad j = p, s. \quad (7)$$

with:

$$t_j^{mdw} = (t_j^{mf} t_j^{fw}) / [\exp(-jk_{zf}d_f) + r_j^{mf} r_j^{fw} \exp(jk_{zf}d_f)] \quad j = p, s. \quad (8)$$

$$r_j^{mdw} = (r_j^{mf} + r_j^{fw} \exp(2jk_{zf}d_f)) / [1 + r_j^{mf} r_j^{fw} \exp(2jk_{zf}d_f)] \quad j = p, s. \quad (9)$$

where k_{zm} stands for $k_0(n_m^2 - n_g^2 \sin^2 \theta_{inc})^{1/2}$, k_{zf} stands for $k_0(n_f^2 - n_g^2 \sin^2 \theta_{inc})^{1/2}$, and the t_j^{ab} and r_j^{ab} , $j=p,s$ are the Fresnel transmission and reflection coefficients for a single interface between medium a and b , with subscript p referring to p-polarized field, s to s-polarized field. When the dipole is at a distance z from the dielectric film/water interface, the exciting electric field intensity will decay as $|T_{j0}|^2 \exp(-z/d)$

with $d^{-1} = 2k_0(n_g^2 \sin^2 \theta_{inc} - n_w^2)^{1/2}$, $j=p,s$ [20]. Assuming a uniform distribution of the orientations of the molecules' absorption dipoles, fluorescence brightness, i.e. the observed fluorescence intensity will be proportional to [18]:

$$|T_j|^2 \langle I_{w,g}(z) \rangle_{\hat{p}} \quad j = p, s. \quad (10)$$

where $\langle \rangle_{\hat{p}}$ refers to averaging over all possible emission dipole orientations. Moreover, subscript w refers to collection through the water [see Eq. (5)], subscript g refers to collection through the glass [see Eq. (4)].

3. Results and discussion

Numerical calculations have been performed for fluorophores that are excited at 532 nm and have their emission maximum at 570 nm. The refractive index of glass substrate was $n_g = 1.51$, whereas an aqueous half space ($n_w = 1.33$) was considered as upper medium. Silver was chosen as a metal, because of its capability to give narrower angular resonances for the metal-clad waveguide modes [21]. The refractive index adopted for the silver was $n_m = 0.1195 + j \cdot 3.5278$ at 570 nm and $n_m = 0.1294 + j \cdot 3.2198$ at 532 nm. Finally, a refractive index of the dielectric film $n_f = 1.49$ was chosen.

First, we studied the possibility to achieve high directionality of fluorescence emission into glass, through coupling with MCLW modes. To this aim, we performed an optimization on silver film thickness and dielectric film thickness, by considering the maximum of $S_{w,g}(\theta, \phi, z=0, \beta) / S_{total}(z=0, \beta)$ while varying θ and ϕ , as the optimization parameter. Results of simulations carried out for a vertical dipole orientation ($\beta = 0$) are shown in Fig. 2. It is seen that maximum photon emission probability density increases rapidly when the thickness of the dielectric film raises above ~ 320 nm, whereas the optimal silver thickness is ~ 46 nm. Remarkably, a value of 46 nm was previously reported as the silver thickness which results in the maximum coupling of fluorescence emission with the surface plasmon (SP), for a silver-coated glass substrate and fluorophores immersed in an aqueous medium, at the emission wavelength of 570 nm [9].

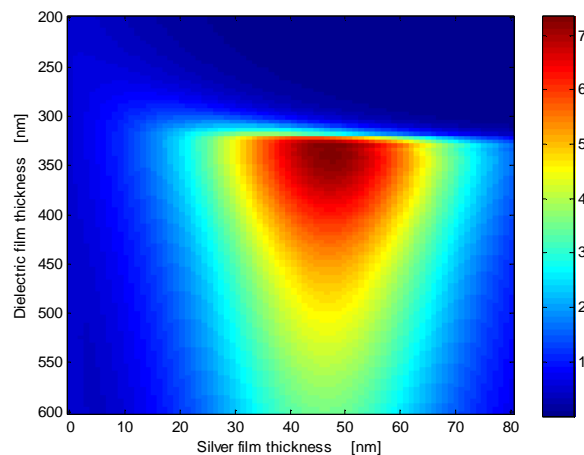


Fig. 2. Maximum fluorescence emission probability density into the glass half space, calculated for a vertically oriented molecule placed at $z = 0$, as a function of the silver film thickness and the dielectric film thickness.

The dependence of fluorescence emission on dielectric film thickness can be understood by studying the modal properties of the MCLW. As a vertically oriented dipole radiates a p-polarized electric field [15], fluorescence emission can couple in this case only with the waveguide TM mode. When the dielectric film thickness is above the cut-off of the fundamental TM mode (~ 317 nm), fluorescence emission couples with the leaky waveguide mode, then being re-radiated over a very narrow angular distribution into the glass, the radiated energy being concentrated around the angle corresponding to the MCLW leaky mode de-coupling angle. To demonstrate coupling between fluorescence emission and MCLW modes, we calculated the effective refractive index of the fundamental TM mode of the MCLW, for a silver thickness of 46 nm, as a function of the dielectric film thickness. Effective refractive indexes were calculated by numerically solving the MCLW dispersion equation given in [21]. The angles corresponding to the real part of the calculated index, N_R ,

calculated as $\theta_{TM} = \sin^{-1}(N_R/n_g)$ are plotted in Fig. 3(a), together with the angular positions of the ADR emission peak into glass.

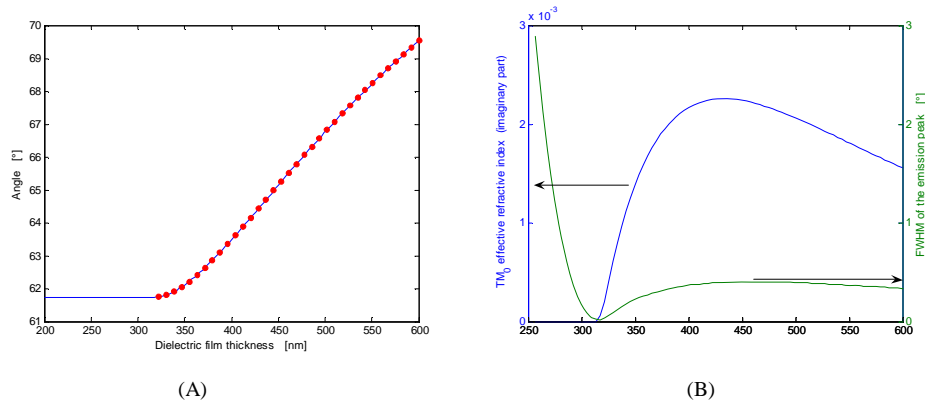


Fig. 3. (a) De-coupling angle into glass of the fundamental TM mode of the MCLW waveguide, calculated for a silver thickness of 46 nm, as a function of the dielectric film thickness (solid line), and angular position of the fluorescence emission peak into glass, for a vertically oriented molecule located directly above the dielectric film (red circles). (B) Imaginary part of the effective refractive index for the fundamental TM mode of the MCLW waveguide, calculated for a silver thickness of 46 nm, as a function of the dielectric film thickness (blue line). On the same plot it is shown the full width at half-maximum (FWHM) of the fluorescence emission peak into glass, for a vertically oriented molecule located directly above the dielectric film (green line).

A similar correspondence is expected between the imaginary part of the effective refractive index (the modal attenuation coefficient due to the energy lost through the glass substrate), with the angular width of the ADR. This is confirmed by the results in Fig. 3(b), which simultaneously shows the calculated attenuation coefficient, and the full width at half-maximum (FWHM) of the ADR. It is interesting to note that the FWHM of the emission peak decreases rapidly when the dielectric film thickness reaches the cut-off, i.e. when coupling with the TM mode of the leaky waveguide occurs. When increasing the dielectric film thickness further, the FWHM slightly increases, reaching a maximum and then starting to decrease. Such a behavior is also observed for the effective index imaginary part. As an example of angular distribution of fluorescence emission, we show in Fig. 4(a) the polar plot of the ADR in water and glass, calculated for $d_m = 46$ nm and $d_f = 340$ nm, for a vertically oriented fluorophore located directly on the dielectric film/water interface.

The above analysis was also performed for a horizontally oriented dipole ($\beta = \pi/2$). The maximum emission probability density into the glass, as a function of dielectric film thickness and silver film thickness is shown in Fig. 5. Still, there is a dielectric film thickness (~ 187 nm) above which a rapid increase in peak emission occurs. This is related to the coupling with the fundamental TE mode of the leaky waveguide. In fact, most of the energy emitted by a horizontally oriented dipole is s-polarized [15].

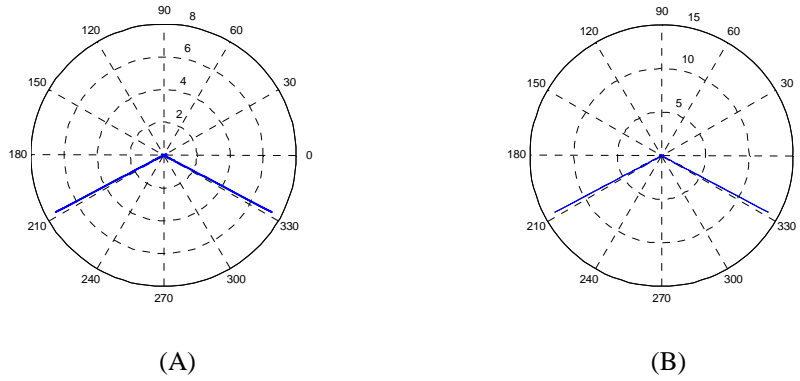


Fig. 4. (A) Angular distribution of emission for a vertically oriented molecule directly on the dielectric film surface, calculated for a silver film thickness $d_m = 46$ nm and a dielectric film thickness $d_f = 340$ nm. (B) Angular distribution of emission for a horizontally oriented molecule directly on the dielectric film surface, calculated for a silver film thickness $d_m = 40$ nm and a dielectric film thickness $d_f = 200$ nm.

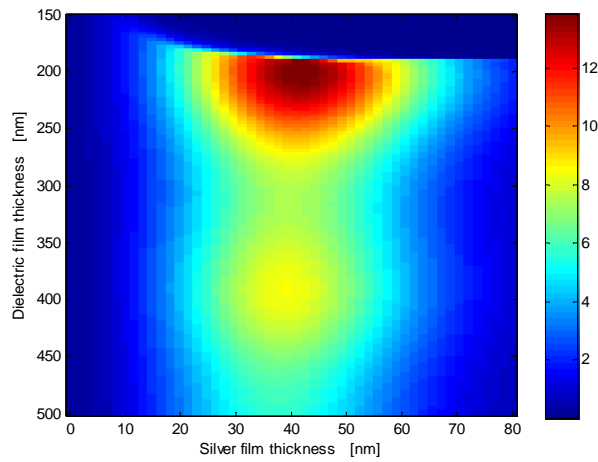


Fig. 5. Maximum fluorescence emission probability density into the glass half space, calculated for a horizontally oriented molecule placed at $z = 0$, as a function of the silver film thickness and the dielectric film thickness.

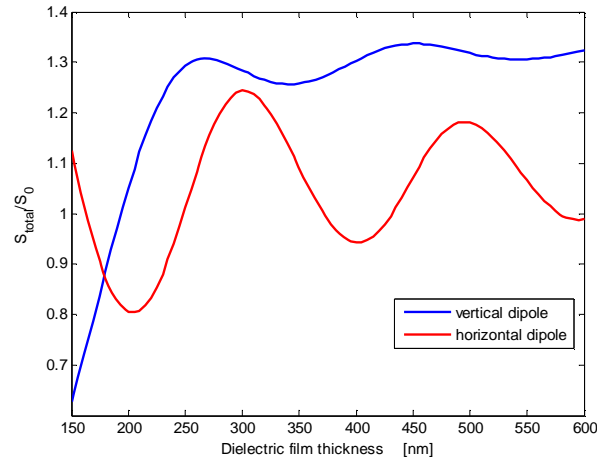


Fig. 6. Total emission rate in presence of the multilayer, normalized to the total emission rate in the free space, as a function of the dielectric film thickness, calculated for a vertically-oriented dipole and $d_m = 46$ nm (blue line), and a horizontally-oriented dipole and $d_m = 40$ nm (red line).

When increasing d_f above ~ 200 nm, maximum peak emission decreases, then increasing again for $d_f > 320$ nm. The second peak, appearing in Fig. 5, is due to a reduction in the total power radiated by the dipole for $d_f \approx 400$ nm. In particular, it turns out that the total power emitted by the dipole is a periodic function of the dielectric film thickness, as it is shown in Fig. 6. As the maximum emission probability is inversely proportional to the total emission rate [see Eq. (4)], such a periodic behavior is also observed in Fig. 5. An explanation of the periodic behavior exhibited by the total emission rate can be found by considering Eq. (3). As discussed above, the power emitted by the dipole is the sum of the power emitted by a free-space dipole, plus a contribution related to the imaginary part of the back-reaction electric field. The latter contribution can either increase or decrease the total emission rate, depending on the distance between the dipole and the reflective metallic film, that is on the dielectric film thickness. The oscillatory behavior of the dipole's total emission rate, with respect to the distance of the dipole from a metallic planar surface has been already reported elsewhere; see, for example, Ref. [11, 17].

Silver thickness providing maximum peak emission is about 40 nm, thus slightly smaller than the optimal thickness found for vertical dipole orientation. As an example, in Fig. 4(b) we report a polar plot of the ADR in water and glass for horizontally oriented dipole placed on the dielectric film/water interface, calculated for $d_f = 200$ nm and $d_m = 40$ nm. Numerical simulations, not shown here, demonstrated for the FWHM of the TE-coupled emission peak, the same dependence on d_f as the FWHM of the TM-coupled emission shown in Fig. 3(b): It reaches an absolute minimum at the cut-off point of the TE mode ($d_f \sim 187$ nm), while increasing for larger values of d_f . The FWHM of the TE-coupled emission peak, calculated for the dielectric film thickness assuring maximum peak emission ($d_f = 200$ nm) is 0.048° , whereas the FWHM due to TM-coupled emission at $d_f = 340$ nm is 0.17° . It is useful to compare these values with the angular width achieved in SPCE, i.e. when emission occurs in absence of dielectric film. By choosing a silver thickness $d_m = 46$ nm, the FWHM of SPCE is 3.38° for a vertically oriented dipole, and 3.39° for a horizontally oriented dipole (the small difference between the two orientations is due to the minor s-polarized fraction of energy emitted by the horizontal dipole). Therefore, coupling of dipole emission with the MCLW modes allows for an emission into glass which is still more directional than SPCE. Another advantage of MCLW-coupled emission is the angular position of the emission peak, which is near the glass/water TIR angle ($\sim 61.7^\circ$) when choosing a dielectric film thickness near the cut-off [see Fig. 3(a)]. This should be compared with the angular position of SPCE, which is

quite higher ($\sim 71^\circ$ for a 46 nm-thick silver film), hence fluorescence signal detection will be more difficult in the latter case. For comparison, we also calculated the FWHM of the emission peak occurring for a pure water/glass interface, i.e. neither dielectric film nor metal film are present. In this case, FWHM is 8.84° for a vertically oriented dipole, and 14.44° for a horizontally oriented dipole.

Besides the directionality of fluorescence emission, another important aspect of fluorescence detection is the fraction of total energy radiated from the dipole, which can be collected through glass, as a function of dipole's distance from the surface. Here we will suppose that the total energy emitted from the dipole on the glass half space is collected. This hypothesis is justified considering that the MCLW can be designed so that emission into glass is concentrated at angles close to the critical angle of TIR, and that high efficiency of collection for emission occurring at angles far above the critical angle of TIR, has been reported for SPCE [5]. Collection efficiency was calculated for a vertically oriented dipole and thicknesses $d_f = 340$ nm, $d_m = 46$ nm [see Fig. 7(a)], and for a horizontally oriented dipole and thicknesses $d_f = 200$ nm, $d_m = 40$ nm [see Fig. 7(b)]. In the same figures, we also report the collection efficiency calculated for SPCE ($d_m = 46$ nm), and for a pure glass/water interface.

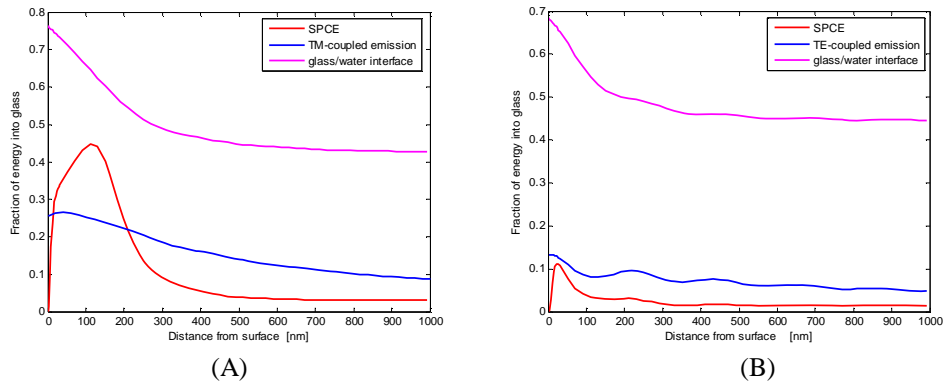


Fig. 7. (A) Fraction of energy radiated into the glass half space by a vertically oriented molecule as a function of the molecule's distance from the surface. The blue line refers to the case of a molecule on a dielectric film/silver film multilayer (MCLW), with a silver thickness of 46 nm and a dielectric film thickness of 340 nm. The red line refers to the case of a molecule on a silver film (surface plasmon-coupled emission - SPCE), with a silver thickness of 46 nm. The magenta line refers to the case of a molecule on a pure glass/water interface. (B) Fraction of energy radiated into the glass half space for a horizontally oriented molecule, as a function of the molecule's distance from the surface. The blue line refers to the case of a molecule on a dielectric film/silver film multilayer (MCLW), with a silver thickness of 40 nm and a dielectric film thickness of 200 nm. The red line refers to the case of a molecule on a silver film (surface plasmon-coupled emission - SPCE), with a silver thickness of 40 nm. The magenta line refers to the case of a molecule on a pure glass/water interface.

From both figures we note that both SPCE and MCLW-coupled emission allow for a smaller fraction of energy emitted into the glass, when compared with the pure glass/water interface. This occurrence is obviously due to the energy dissipation in the metal, which affects both SPCE and MCLW configurations. For MCLW-coupled emission, the highest efficiency with which the excited state energy is emitted into glass occurs for a vertical dipole orientation and a dipole's distance of ~ 43 nm from the dielectric film. Even under such ideal conditions, the energy lost in the metal is nearly the same as the energy emitted as TM-coupled emission ($\sim 23\%$), while the remaining 54% is emitted into the water half space. Hence, the high directionality provided by MCLW-coupled emission comes at the price of a reduced collection efficiency, with respect to traditional fluorescence detection carried out on a bare glass/water interface. However, we must note that, in the case of pure glass/water

interface and collection for angles above the supercritical angle (SAF detection), collection efficiency becomes actually comparable to collection efficiency offered by MCLW and SPCE [9]. Moreover, MCLW-coupled emission has the advantage that the dielectric film separates the fluorescing molecules from the silver surface, so that collection efficiency does not vanish when the dipoles are placed directly above the MCLW surface. This is in contrast with SPCE, where the energy radiated from the dipole is completely dissipated into the metal when the dipole is placed directly above the metal surface [17, 18].

As a next step, the fluorescence brightness was calculated, by considering both fluorescence excitation and collection from the glass side. To this aim, we first calculated the dependence of the square modulus of the transmission coefficient $|T_{j0}|^2$, $j = p, s$ for a plane wave incident from the glass side onto the metal film, upon the incidence angle, the silver film thickness d_m , and the dielectric film thickness d_f at the excitation wavelength $\lambda_{\text{exc}} = 532$ nm. We plot in Figs. 8(A) and 8(B) the maximum transmission coefficient, calculated by varying the angle of incidence of the exciting field, for p-polarized excitation and s-polarized excitation, respectively, as a function of d_f and d_m .

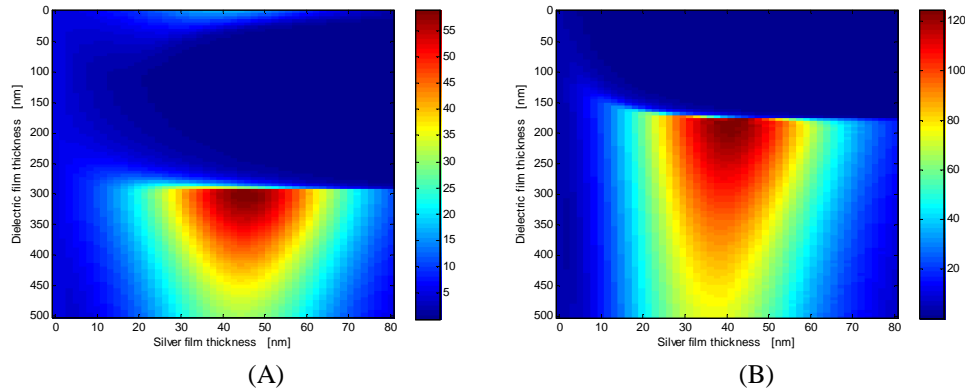


Fig. 8. (A) Maximum transmission coefficient $|T_p|^2$ through the MCLW for a p-polarized plane wave incident from the glass side, as a function of the silver film thickness and the dielectric film thickness. (B) Maximum transmission coefficient $|T_s|^2$ through the MCLW for an s-polarized plane wave incident from the glass side, as a function of the silver film thickness and the dielectric film thickness.

First, we note that illuminating from the glass side may result in an excitation enhancement which can be much higher than the 4-fold improvement reported in [22] for excitation from above (in Ref. [22], a structure very similar to the one depicted in Fig. 1 was considered, consisting of a dielectric film placed above a metallic mirror). Moreover, it is seen that the p-polarized illumination efficiency is maximum when the silver film thickness is 46 nm, which is the same value which resulted in the maximum coupling between fluorescence emission and the MCLW TM mode. Similarly, in the case of s-polarized excitation, the optimal silver thickness is 40 nm, which is the same thickness which provided maximum coupling with the MCLW TE mode. As regards dielectric film thickness, maximum excitation occurs in both cases for a dielectric film thickness slightly smaller than those found from Figs 2 and 5. In particular, maximum excitation occurs for $d_f \sim 300$ nm for p-polarization, and $d_f \sim 190$ nm for s-polarization. Differences with the thicknesses found when optimizing the collection efficiency arises from the two different wavelengths considered for the simulations (532 nm for excitation and 570 nm for collection). We chose to set the dielectric film thicknesses to the values providing maximum fluorescence collection efficiency, and supposed to employ p-polarized illumination in the case of TM-coupled emission ($d_f = 340$

nm, $d_m = 46$ nm), while using s-polarized illumination in the case of TE-coupled emission ($d_f = 200$ nm, $d_m = 40$ nm). In both cases, we assumed plane wave illumination from the glass side, at the incident angle providing maximum excitation. Random orientation of the fluorescing molecules was also assumed, so that fluorescence collection efficiency was calculated as a weighted sum of efficiency for vertical and parallel dipole orientation (one-third vertical orientation plus two-thirds parallel orientation). Fluorescence brightness has been then calculated by using Eq. (10), i.e. by multiplying the maximum transmission coefficient and the fluorescence collection efficiency, for a range of dipole's distances from the MCLW surface. Results are shown in Figs. 9(A) and 9(B). For comparison, we also show in the same figures the results achieved for a pure glass/water interface, both in the case of collection over all the glass half space, and in the case of collection above the supercritical angle (SAF detection). SPCE results are reported only for p-polarized excitation, as in the case of s-polarized excitation the exciting field is so low that maximum brightness was $\sim 4 \cdot 10^{-3}$. Both figures indicate that MCLW-coupled emission allows for a stronger fluorescence signal to be detected through the glass, when compared to both SPCE and pure glass/water interface, for dipoles close to the MCLW surface. Remarkably, a 4-fold improvement is observed for the MCLW configuration, with respect to the glass/water configuration, when exciting with an s-polarization and collecting in both cases over the whole glass half space, while an 8-fold improvement is observed with respect to SAF detection. Comparing Fig. 9 and Fig. 7, it can be seen that the reduced collection efficiency of MCLW-coupled emission with respect to the emission in presence of a pure glass/water interface, is overwhelmed by the strong enhancement of excitation efficiency (see Fig. 8), eventually resulting in a stronger fluorescent signal, at least for molecules placed not too far from the MCLW surface.

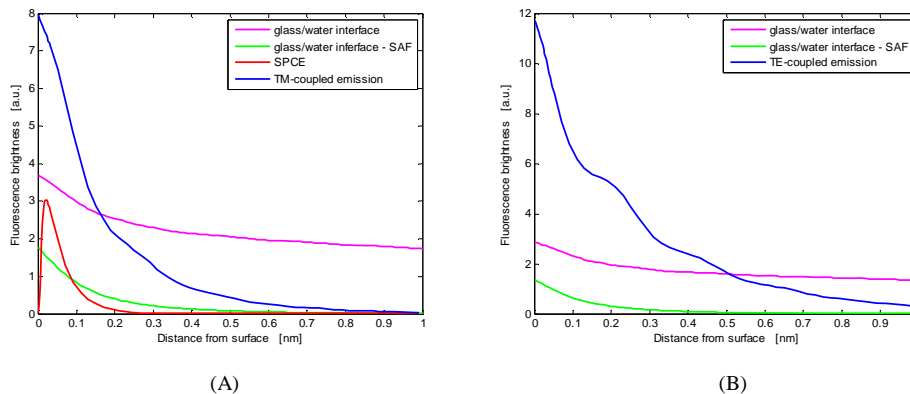


Fig. 9. (A) Maximum detectable fluorescence intensity for s-polarized plane wave excitation from the glass side at the incident angle giving maximum electric field intensity at $z = 0$, when collecting over the whole glass half space, as a function of the molecule's distance from the surface. The blue line refers to the case of a molecule on a dielectric film/silver film multilayer (MCLW), with a silver thickness of 40 nm and a dielectric film thickness of 200 nm. The magenta line refers to the case of a molecule on a pure glass/water interface. Fluorescing molecules are randomly oriented. The green line refers to SAF detection. The red line refers to SPCE with a silver thickness of 40 nm. (B) Maximum detectable fluorescence intensity for p-polarized plane wave excitation from the glass side at the incident angle giving maximum electric field intensity at $z = 0$, when collecting over the whole glass half space, as a function of the molecule's distance from the surface. The blue line refers to the case of a molecule on a dielectric film/silver film multilayer (MCLW), with a silver thickness of 46 nm and a dielectric film thickness of 200 nm. The magenta line refers to the case of a molecule on a pure glass/water interface. The green line refers to SAF detection. Fluorescing molecules are randomly oriented.

From Figs. 9A and 9B, note also the increased range of dipole's distances for which a sufficient fluorescent signal can be detected in the MCLW configuration, with respect to

SPCE and SAF detection. This increased range, which is related, for duality, to the deeper evanescent field of MCLWs exploited in evanescent field sensing, can be an useful property when fluorescence from large emitters has to be detected, such as bacteria, or proteins [12].

Numerical analyses have been carried out so far, by supposing that fluorescence were collected through the glass. Let us now suppose that fluorescence light detection is carried out through a microscope objective immersed into water looking from above. In this case, Eq. (6) must be considered in the calculation of collection efficiency, instead of Eq. (5). We repeated the calculation of fluorescence brightness, as a function of the silver thickness and the dielectric film thickness, in both cases of p-polarized excitation and s-polarized excitation from the glass side. For each calculation, we still suppose an angle of incidence of the exciting field resulting in the maximum electric field intensity at $z = 0$. Fluorescence brightness calculated for $z = 0$ is shown in Figs. 10(a) and 10(b) for p-polarized excitation and s-polarized excitation, respectively.

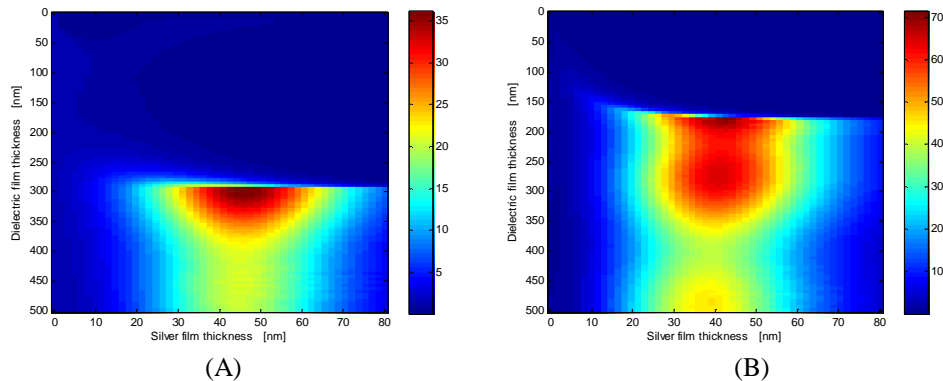


Fig. 10. (A) Maximum detectable fluorescence intensity for p-polarized plane wave excitation from the glass side at the incident angle giving maximum electric field intensity at $z = 0$, when collecting through a water-immersed microscope objective with numerical aperture $NA = 1.3$, as a function of the silver film thickness and the dielectric film thickness. Fluorescing molecules are randomly oriented. (B) Maximum detectable fluorescence intensity for s-polarized plane wave excitation from the glass side at the incident angle giving maximum electric field intensity at $z = 0$, when collecting through a water-immersed microscope objective with numerical aperture $NA = 1.3$, as a function of the silver film thickness and the dielectric film thickness. Fluorescing molecules are randomly oriented.

It is seen that, for fluorescence detection from the microscope objective, maximum brightness is achieved for the same silver thicknesses as determined in the case of collection through the glass, whereas optimal dielectric film thicknesses are slightly smaller than those previously found. In particular, the highest brightness is achieved for s-polarized excitation, a metal film thickness of 40 nm, and a dielectric film thickness of 175 nm. We underline that the 175 nm optimal thickness is the result of a combination of the excitation efficiency, which is maximum for ~ 190 nm dielectric film thickness [see Fig. 8(b)], and collection efficiency which is higher for thicknesses slightly smaller than 190 nm. The oscillatory behavior of fluorescence intensity as a function of the dielectric film thickness, clearly observed in Fig. 10(b), results from a periodic change in collection efficiency. Such a periodic change in collection efficiency comes in this case from two effects: The first one is related to the back-reaction field, leading to a modulation of the total dipole emission rate (see Fig. 6); The second one arises from the interference between the field radiated by the dipole directly toward the objective, and the field radiated by the dipole in the glass' direction and reflected back from the multilayer. We also note that a dielectric film thickness of 175 nm implies that all modes of the MCLW are in cut-off, so that no coupling with the MCLW leaky modes is possible in this case. When the film thicknesses are set to these optimal values ($d_m = 40$ nm and $d_f = 175$ nm), fluorescence brightness is more than 70 times the brightness observed for a

pure glass/water interface. A so dramatic improvement in signal strength, with respect to fluorescence measurement carried out on a standard glass slide, mostly comes from the strong enhancement of the local exciting field when illuminating from the glass side (see Fig. 8). However, also collection efficiency is enhanced by the presence of the multilayer. Actually, by using the above determined optimal thicknesses, it turns out that the major part of dipole's emission is directed into the water half space. In particular, we calculated $I_w^\perp = 56.1\%$ and $I_g^\perp = 6.6\%$ for vertical dipole orientation, $I_w^\parallel = 61.1\%$ and $I_g^\parallel = 4.2\%$ for horizontal dipole orientation. This is in contrast with the case of a dipole emitting at a glass/water interface, for which it is a well-known fact that emission is mostly directed into the glass half space [23]. Indeed, the energy fractions calculated for a pure glass/water interface and $z = 0$ are $I_w^\perp = 21\%$, $I_g^\perp = 79\%$ for vertical dipole orientation, and $I_w^\parallel = 30.3\%$, $I_g^\parallel = 69.7\%$ for horizontal dipole orientation. On the other hand, it must be pointed out that in the case of collection through a microscope objective looking from above, fluorescence emission does not exhibit the property of strong directionality as emission into glass. To show this, a polar plot of the ADR in water and glass for a MCLW having the optimal thickness previously found ($d_m = 40$ nm and $d_f = 175$ nm), in the case of vertical (blue line) and horizontal (red line) dipole, is shown in Fig. 11.

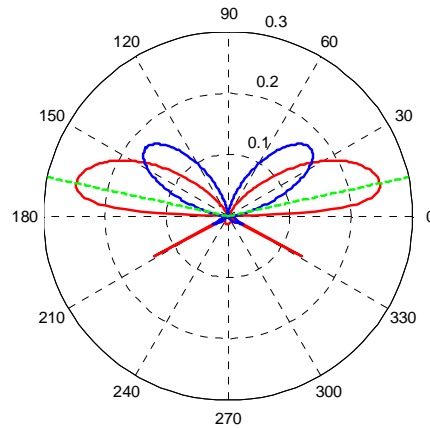


Fig. 11. Angular distribution of emission for a molecule directly on the dielectric film surface, calculated for a silver film thickness $d_m = 40$ nm and a dielectric film thickness $d_f = 175$ nm. The blue line refers to a vertically oriented molecule, whereas the red line refers to a horizontally oriented molecule. The green lines in the plot delimit the cone of light captured by the water-immersed microscope objective with numerical aperture $NA = 1.3$.

It is seen that radiation emitted in the water half space is spread over a wider angular region. Hence, detecting the fluorescence from above permits on one hand to increase collection efficiency, as a higher fraction of energy can be directed into the water half space, rather than into the glass half space. On the other hand, the strong ADR directional properties characterizing emission into the glass half space are lost in this case. Consequently, this detection configuration reduces the utility of the method, because it may greatly reduce any spatial information imparted via evanescent excitation through the inner filtering mechanism previously shown.

4. Conclusions

Fluorescence emission in presence of a multilayer formed by a thin dielectric film and a thin metal film deposited above a glass substrate, has been theoretically studied. We have shown that, by opportune design of the multilayer, an extremely narrow angular distribution of fluorescence emission into the glass substrate can be achieved. It has been also shown that the angular distribution of emission into glass can be studied by analyzing the multilayer as a leaky metal-clad waveguide (MCLW), and studying its modal properties. When the MCLW is designed to support one leaky mode, fluorescence emission into glass is concentrated around a very specific angle related to the real part of the corresponding MLCW mode effective index. In particular, peak emission into glass can be maximized by choosing the dielectric film thickness so as to operate the MCLW near its TE mode cut-off point.

Although the presence of the metal film inevitably results in a certain degree of energy dissipation, it has been shown that illuminating the MCLW from the glass side, a fluorescence brightness (i.e. signal strength) higher than the brightness achievable for surface-plasmon coupled emission (SPCE) and classical glass/water emission can be achieved, when fluorescence is collected through the substrate. As MCLW-coupled emission has been demonstrated to be still more directional than SPCE, this may help to better discriminate between fluorescence and any other background. We have also shown that a dramatic increase (~ 70 -fold) in fluorescence signal can be achieved using the MCLW, with respect to classical fluorescence detection scheme carried out on a standard glass slide, by collecting the fluorescence from above through a light-collecting microscope objective and illuminating from the glass side at an optimal angle of incidence.